ISSN:1991-8178

Australian Journal of Basic and Applied Sciences

Journal home page: www.ajbasweb.com

Independent Component Analysis and Uncorrelated Discriminant Analysis for Diabetic Retinopathy Lesion Detection

[1]Sirajudeen, A. and [2]Dr. Ezhilarasi, M.

[1]*Electronics and Communication Engineering Department, RVS Technical Campus - Coimbatore, Faculty of Engineering, Anna University, Coimbatore, Tamilnadu, India.*
[2]*Electronics and Instrumentation Engineering Department, Kumaraguru College of Technology, Anna University, Coimbatatore, Tamilnadu, India.*

ARTICLE INFO

Article history:
Received 12 November 2014
Received in revised form 26 December 2014
Accepted 29 January 2015
Available online 10 February 2015

Keywords:
Diabetic Retinopathy, Exudates, Hemorrhage, Microaneurysms, Neovascularization Automatic screening, ICA, UDA.

ABSTRACT

Background: In the field of medical sciences, identification of Diabetic Retinopathy is one of the most challenging tasks. Most of the methods used require the development of specific segmentation techniques for finding each abnormality on the retina. **Objective:** we propose the use of Independent Component Analysis in order to differentiate between the normal and infected retinal images which highly reduce the second-order and higher-order dependencies in the input. We use the standard images which are used in the study of diabetic treatments and concentrate on various types of lesions related to diabetic retinopathy. **Results:** The ICA reduces the dimensionality of the input images and hence produces better result compared to that of the previous PCA versions of Diabetic Retinopathy Lesion Detection. The results obtained clearly shows the distinction between the normal retinal structures and affected retinal structures. **Conclusion:** ICA method could be clearly applied for identification of Diabetic Retinal Lesions. Also, it is proved that UDA is more efficient than ICA.

To Cite This Article: Sirajudeen, A. and Dr. Ezhilarasi, M., Independent Component Analysis and Uncorrelated Discriminant Analysis for Diabetic Retinopathy Lesion Detection. ***Aust. J. Basic & Appl. Sci.,*** *9(5): 238-244, 2015*

INTRODUCTION

Diabetic Retinopathy is one that could cause permanent blindness to the eyes. The occurrence varies with period in which a person is subjected to diabetes. Usually color fundus images are used by doctors to study this (Bishop C.M., 1995). The identification of Diabetic Retinopathy is one of the most tedious and challenging tasks in the domain of Medical Sciences. In most cases detection of diabetic retinopathy involves the segmentation of the image into a number of minute parts to separate the abnormalities found in the retina. Various Image Processing techniques are being used to identify the Diabetic Retinopathy. But still, in some cases, the identification may not be accurate. In this paper, we propose a method which employs the AM-FM decomposition along with Independent Component Analysis to normalize most of the approximations that are being made in previously used techniques. Fig. 1 shows normal and various Diabetic Retinopathy images.

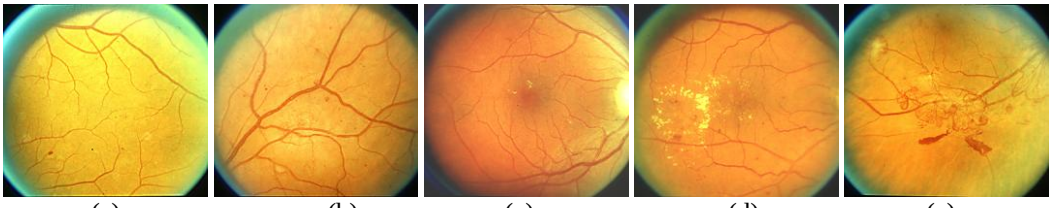

(a) (b) (c) (d) (e)

Fig. 1: (a) Normal Retina , (b) Neovascularization, (c) Microaneurysms, (d) Exudates, (e) Hemorrhage.

Previously various techniques were used to detect the occurrence of Diabetic Retinopathy. In (Cover, T.M. and J.A. Thomas, 1991), a system based on color normalization and local contrast enhancement is being used to detect the exudates. This is an initial work done by Osareh which

Corresponding Author: Sirajudeen, A., Electronics and Communication Engineering Department, RVS Technical Campus - Coimbatore, Faculty of Engineering, Anna University, Coimbatore, Tamilnadu, India.

happened to make certain wrong identifications and predictions. In (Christopher Hann, 2009), a non-invasive transient visual evoked potential phase spectral components periodicity measure based method to classify diabetic retinopathy is being employed.

Use of threshold and region growing methods were used to detect exudates (Gunturk, B.K., 2003; Jin, Z., 1999), use a median filter to remove noise, segment bright lesions and dark lesions by threshold. perform region growing, then identify exudates regions with Bayesian, Mahalanobis, and nearest neighbor (NN) classifiers. Recursive region growing segmentation (RRGS) (Jin, Z., 2001) have been used for an automated detection of diabetic retinopathy Adaptive intensity threshold and combination of RRGS were used to detect exudates (Liu, Chutatape, Krishna, 1997; Lawrence, S.,1193), combine color and sharp edge features to detect exudate. First they find yellowish objects, and then they find sharp edges using various rotated versions of Kirsch masks on the green component of the original image. Yellowish objects with sharp edges are classified as exudates.

Methods:

1.1 Database:

The experimentation is done using the ETDRS Database. The following six categories are taken into consideration for the experimentation: MAs, hemorrhages, exudates, neovascularization (NV), retinal background and vessels.

The following are the steps involved in our process.

1.2 AM-FM Decomposition:

An image can be approximated by a sum of AM-FM components given by

$$I(x,y) \approx \sum_{n=1}^{M} a_n(x,y)\cos\varphi_n(x,y)$$

where,

M - No. of AM-FM components

$a_n(x,y)$ - Instantaneous Amplitude (IA) functions

$\varphi_n(x,y)$ - Instantaneous Phase functions

Here we focus on the AM-FM textures. The Instantaneous Frequency(IF) is defined in terms of gradient of the phase φ_n as

$$\nabla\varphi_n(x,y) = \left(\frac{\partial\varphi_n(x,y)}{\partial x}, \frac{\partial\varphi_n(x,y)}{\partial y}\right)$$

For feature extraction, we use IF and IA. IF measures the local frequency content and is independent of any image rotations or retinal imaging hardware characteristics. IF magnitude is the measurement of the geometry of the texture with strong degree of independence from contrast and non-uniform illumination variations. Here, we use relative angles which are estimated locally as derivations from the dominant neighborhood angle. Therefore, the blood vessels will provide a relative angle around zero. The relative angle may have a range from $-\pi/2$ to $\pi/2$. Therefore sign ambiguity may arise. That is $\cos\varphi(x,y)$ represents the same as $\cos[-\varphi(x,y)]$. Local image intensity variations including edges are reflected in IA.

1.3 Frequency Scale and Filter Banks:

The AM-FM components are extracted from different image scales. Consider the usage of 25 bandpass filters associated with 4 frequency scales and 9 possible Combination of Scales (CoS). Estimate AM-FM component over each combination of scales using Dominant Component Analysis (DCA). At lower frequency scales, the magnitude values of |IF| are small and the extracted AM-FM features reflect slowly the varying image textures. The usage of different scales also considers size variability among structures such as MAs, exudates, hemorrhages etc. For Diabetic Retinopathy patients, the lesion size varies. The dark lesions which are found may be termed Mas and the light lesions may be termed exudates. The various filters which are being used consider the orientation of the features which are being encoded. The frequency ranges of the band pass filters are shown in table 1.

Table 1: Bandpass filters associated with Multiple Image Scales.

Frequency Scale Band	Filters	Instantaneous Wavelength (period) Range in Pixels	Range in mm
Low Pass Filter (LPF)	1	22.6 to ∞	0.226 to ∞
Very Low Frequencies (VL)	20-25	11.3 to 32	0.113 to 0.32
Low Frequencies (L)	14-19	5.7 to 16	0.057 to 0.16
Medium Frequencies (M)	8-13	2.8 to 8	0.028 to 0.08
High Frequencies (H)	2-7	1.4 to 4	0.014 to 0.04

1.4 Encoding the structures using AM-FM:

To characterize the retinal structures, the Cumulative Distribution Functions (CDFs) of the IA, |IF| and the relative angle are used. Since the range of values of each estimate varies according to the CoS used, the histograms are computed from the global minimum to the global maximum.

A region with small pixel intensity variation will also be characterized by low IA values in a higher frequency scales. This is due to the concept that low intensity variation regions will also contain weak-frequency components. Darker regions will have low IA values in the lower frequency scales.

The magnitude of IF is insensitive to the direction of image intensity variations. This may

make it easier to identify exudates which are present along with MAs.

1.5 Procedure to find Mahalanobis Distance:

Initially, the features for a particular region are extracted. Then, the dimensionality is reduced using Independent Component Analysis (ICA) after which the mean of a collection of regions corresponding to a specific lesion is found. The ICA reduces the noise as well the dimensionality of the image. Initially, we consider a statistical model

$y = Ax$

where x is considered a random vector with m independent components. A is an $m \times m$ matrix of invertible parameters. y is considered an observed vector with m components. Based on a set of N independent, identically distributed observations of the vector y which we wish to estimate the parameter matrix A. From the estimate of A we can estimate the values of x corresponding to any observed y by solving a linear system of equations. The distribution of x is unknown. The maximum likelihood of A need to be estimated. Consider the population version of ICA in which $p^*(y)$ denotes the true distribution of y and $p(y)$ denotes the model. The Kullback-Leibler (KL) divergence between the distributions is minimized as $D(p^*(y) \| p(y))$. Define $W = A^{-1}$, so that $x = Wy$. Since the KL divergence is invariant with respect to an invertible transformation, the problem is set equivalent to minimization of $D(p^*(x) \| p(x))$. Let $\tilde{p}(x)$ denote the joint probability distribution obtained by taking the product of the marginal of $p^*(x)$. We have the following decomposition of the KL divergence (Lawrence, S., 1993).

$D(p^*(x) \| p(x)) = D(p^*(x) \| \tilde{p}(x) \| p(x))$, for any distribution $p(x)$ with independent components. Consequently, for a given A, the minimum over all possible $p(x)$ is attained precisely at $p(x) = \tilde{p}(x)$ and the minimal value is $D(p^*(x) \| p(x))$ which is exactly the mutual information between the components of $x = Wy$. In such a way, six means are found out. From the six means, the Mahalanobis distance is estimated. The procedure is clearly described in Fig. 2.

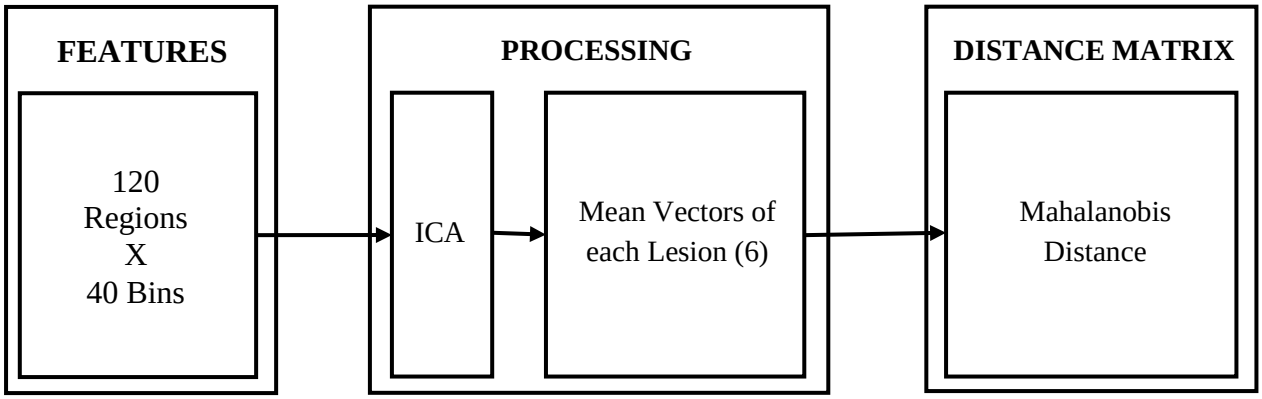

Fig. 2: Finding Mahalanobis Distance.

1.6 Classification of Retinal Images using ICA:

Fig. 3 shows the steps involved in the classification of the retinal images. Initially the features are extracted using AM-FM. The reduction of dimensionality is done using ICA. Further, the dimensionality is reduced using k-means clustering. Finally, Pixel Level Snakes (PLS) is applied to classify the images.

1.7 Alternate solution using UDA (Uncorrelated Discriminant Analysis):

The above proposed solution could also be replaced by Uncorrelated Discriminant Analysis (UDA). The change is made in the reduction of dimensionality of the original image after being encoded using AM-FM reduction.

1.7.1 Fisher Vector:

Suppose $\omega_1, \omega_2, \ldots\ldots, \omega_L$ are L known pattern classes. Let the set of x be considered X which is an N -dimensional sample. Suppose $m_i, S_i, P_i (i = 1,2,\ldots\ldots,L)$ are mean vector, the covariance matrix and a priori probability of class ω_i respectively. The between-class scatter matrix S_w and the total population scatter matrix S_t are determined by the following formulae:

$$S_b = \sum_{i=1}^{L} P_i [m_i - E(X)][m_i - E(X)]^T ,$$

$$S_w = \sum_{i=1}^{L} P_i E[(X - m_i)(X - mi)^T \mid \omega_i] = \sum_{i=1}^{L} P_i S_i$$

$$S_t = E\{[X - E(X)][X - E(X)]^T\} = S_b + S_w$$

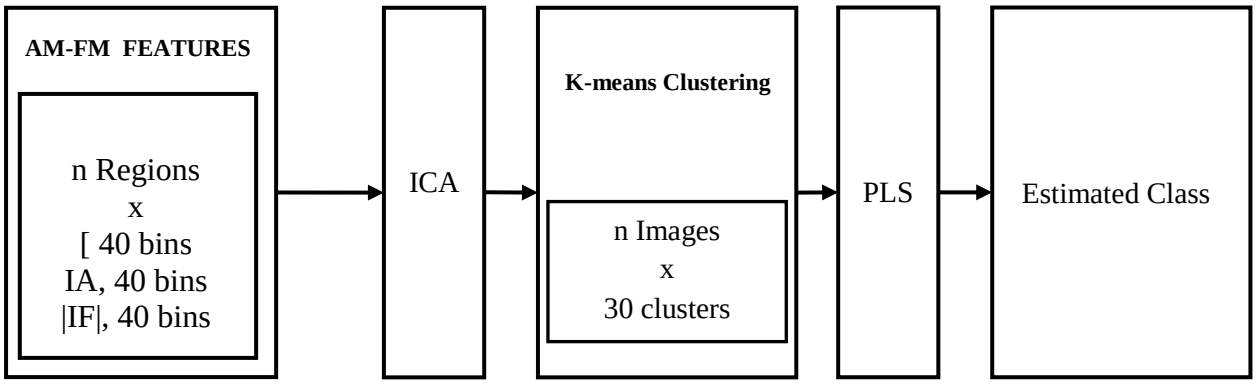

Fig. 3: Classification of Retinal Images.

According to the scatter matrices, the Fisher criterion function can be defined as follows:

$$F(\varphi) = \frac{\varphi^T S_b \varphi}{\varphi^T S_w \varphi}$$

where φ is an arbitrary vector in N-dimensional space $\Re_N$.

The vector φ_1 corresponding to maximum of $F(\varphi)$ is the Fisher optimal discriminant direction or the Fisher vector.

1.7.2 Uncorrelated discriminant vectors: [9]

Let φ_1 be Fisher's vector. Suppose j directions $\varphi_1, \varphi_2, ...\varphi_r (r \geq 1)$ are obtained. In order to obtain uncorrelated discriminant features, we can let the $(r+1)^{th}$ direction φ_{r+1} which maximizes the Fisher criterion function $F(\varphi)$ with the following conjugated orthogonality constraints:

$$\varphi_r^T +_1 S_t \varphi_i = 0 \qquad (i = 1,2,..r)$$

The above constraints can be combined with the formula below.

$$Y = \begin{bmatrix} y_1 \\ y_2 \\ . \\ . \\ y_k \end{bmatrix} = \begin{bmatrix} \varphi_1^T \\ \varphi_2^T \\ . \\ . \\ \varphi_k^T \end{bmatrix} X$$

The above transformation along with the constraint is called as uncorrelated discriminant transformation.

1.7.3 Uncorrelated Feature Extraction [10]:

Feature extraction consists of choosing those features which are the most elective for preserving and increasing class separability. Suppose there are L known face classes. Let face images have a resolution $m \times n$ and then the dimensionality of the original space is $N = mn$. Let K be the number of training samples. If the resolution $m \times n$ is so low that $K > N + L$ the uncorrelated discriminant transformation can be directly used to extract features of face images with the following three steps:

Step A: Calculate the $N \times N$ between-class scatter matrix S_b, the $N \times N$ within-class scatter matrix S_w and $N \times N$ the total population scatter matrix in the original X-space $\Re_N$ with K training samples.

Step B: Calculate all the N-dimensional uncorrelated discriminant vectors $\varphi_1, \varphi_2, ...\varphi_k$,the number of which is the minimum of N and (L-1) i.e.
k=min(*N*,*L-1*)

Step C: perform the linear transform from the original X-space $\Re_N$ to the uncorrelated discriminant feature Y-space $\Re_k$.

With these steps performed the features of the image are extracted. From the six means, the Mahalanobis distance is estimated by using UDA method. The procedure is clearly described in Fig. 4.

1.8 Classification of Retinal Images using UDA:

Fig. 5 shows the steps involved in the classification of the retinal images. Initially the features are extracted using AM-FM. The reduction of dimensionality is done using ICA. Further, the dimensionality is reduced using k-means clustering. Finally, Pixel Level Snakes (PLS) is applied to classify the images.

RESULTS AND DISCUSSION

The experimentation shows the impact of the Independent Component Analysis over the AM-FM feature extraction. The ETDRS database is used for the purpose of analysis. The proposed system which uses ICA is experimented against the existing systems which use PCA. In addition, it also involves the analysis of a system using UDA also. The analysis is done based on the level of accuracy based on Mahalanobis Distance and Hellinger Distance.

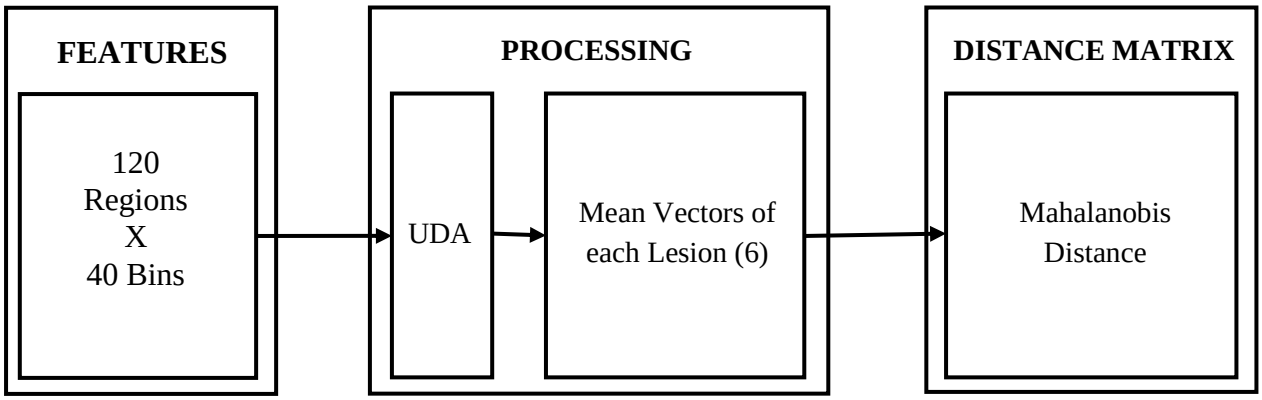

Fig. 4: Finding Mahalanobis Distance using UDA.

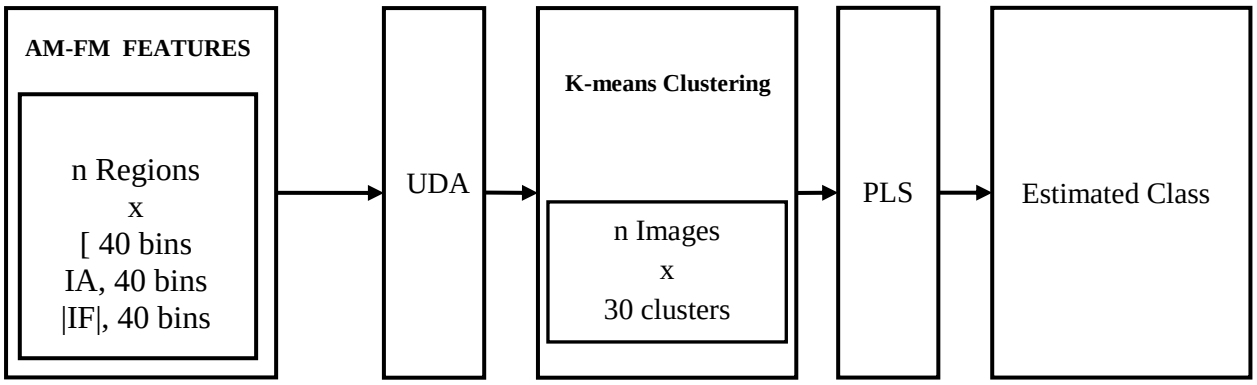

Fig. 5: Classification of Retinal Images using UDA.

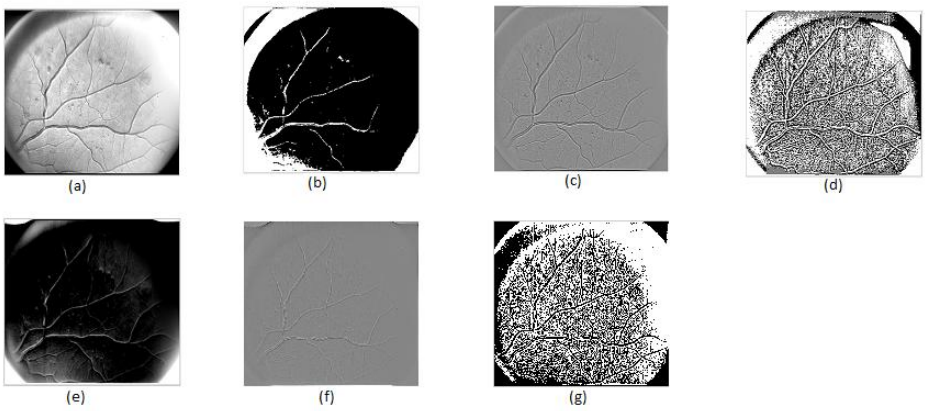

Fig. 6: (a) IA using medium, low and very low frequencies, (b) Threshold image, (c) IA using low frequencies, (d) Threshold image, (e) Instantaneous Frequency, (f) IF magnitude using low-pass filter, (g) AM-FM Decompositions

Fig. 6 shows the various changes that occur in the retinal image which is given as input. It is only with the background of these changes, the system is able to find whether the given input is subjected to diabetic retinopathy or not. Fig. 7 shows the various features that are being used for the purpose of identification of diabetic retinopathy.

Fig. 8 (a) shows the original image. Fig. (b) shows by using Principal Component Analysis (PCA) method, the output image is not affected by Diabetic Retinopathy. Fig. (c) shows by using Independent Component Analysis (ICA) method, the output image is Non Diabetic Retinopathy. As in Fig. (d) system shows by using Uncorrelated Discriminant Analysis (UDA) method, the output image is affected by Diabetic Retinopathy.

The Mahalanobis Distance shows the dissimilarity measure between two vectors p and q with covariance matrix S as

$$d(p,q) = \sqrt{(p-q)^T S^{-1}(p-q)}$$

It could be found that the system using ICA for feature classification is much more accurate than the system using PCA based on Mahalanobis Distance. However, ICA is less accurate than UDA. But comparing the cost in terms of time and space, it is found that ICA suits economically when used in any system rather than that of UDA. The accuracy of ICA is mainly due to the process of whitening which reduces the dimensionality to a tremendous level without reducing the quality of the textures in an image. This makes it provable that ICA is better than PCA in most cases. The same level of result could also be observed in the comparison of accuracy based on Hellinger distance also.

Fig. 7: Identification of diabetic retinopathy (a) Exudates, (b) Neovascularization, (c) Microaneurysms, (d) Hemorrhages, (e) Vessels and (f) Retinal background.

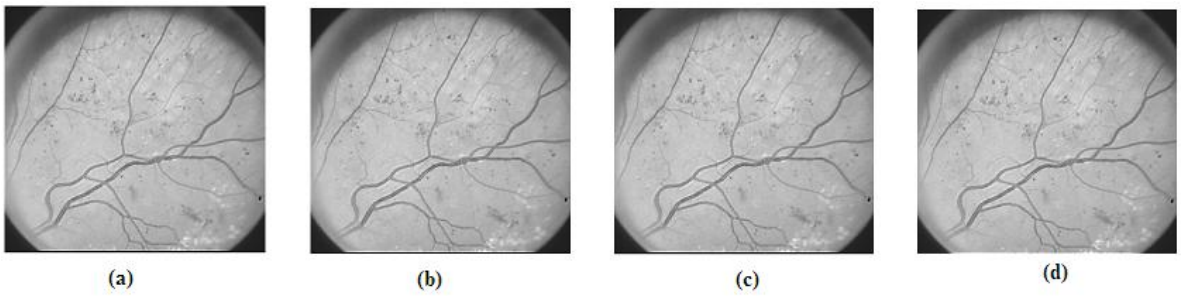

Fig. 8: Varied Outputs (a) Original input image, (b) PCA method - Non-DR image, (c) ICA method – Non-DR image, (d) UDA method - DR image

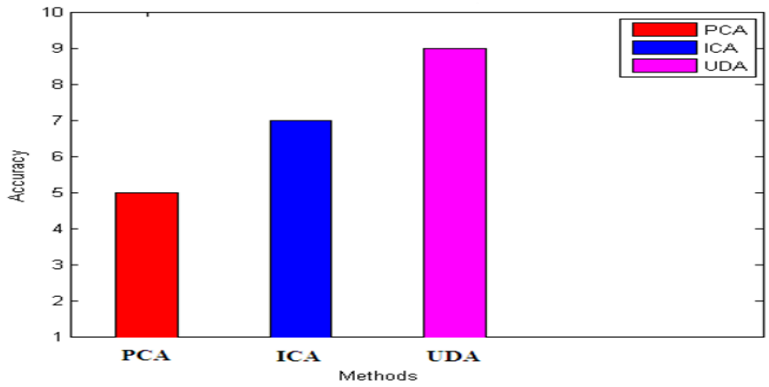

Fig. 9: Accuracy level of Hellinger Distance.

If p and q are the probability measures and λ another measure, the Hellinger distance is defined as

$$H^2 = \frac{1}{2}\int\left(\sqrt{\frac{dp}{d\lambda}} - \sqrt{\frac{dq}{d\lambda}}\right)^2 d\lambda$$

It is already evident from the results obtained based on the Mahalanobis distance that ICA is more accurate than PCA. The results obtained based on the Hellinger distance adds proof to the same. This experimentation also provides the same type of result placing ICA in between PCA and UDA. It is better to use ICA since it provides a considerable level of accuracy. However UDA can be used for better results.

Table 2: Hellinger Distance (1.0e+032*).

Lesions	Exudates	RB	MAs	HE	NV	Vessels
Exudates	0.0000	2.8341	1.7975	6.5766	8.9955	4.8939
RB	2.2267	0.0000	2.8764	5.4102	9.4459	5.1560
MAs	1.2164	2.4777	0.0000	6.3519	9.3982	4.8220
HE	3.1093	3.2557	4.4375	0.0000	5.3536	5.6983
NV	2.4904	3.3286	3.8447	3.1350	0.0000	4.5214
Vessels	2.1125	2.8328	3.0756	5.2025	7.0495	0.0000

Conclusion:

In this paper, the Independent Component Analysis is being introduced into the process of detecting Diabetic Retinopathy. A replacement in the system, where PCA was used is done using ICA. The experimentations made, proved that the application of ICA inside the system provided a much more accurate result compared to that which uses PCA. Moreover, UDA is proven to be more accurate than ICA.

ACKNOWLEGEMENT

The authors would like to thank Méthodes d'Evaluation de Systèmes de Segmentation et d'Indexation Dédiées à l'Ophtal-mologie Rétinienne for allowing them to use their database in this study.

REFERENCES

(21.01.2014).
http://messidor.crihan.fr/download-en.php.

Bishop C.M., 1995. "Neural Networks for Pattern Recognition" London, U.K.: Oxford University Press.

Christopher Hann, James Revie, Darren Hewett, Geoffrey Chase and Geoffrey Shaw 2009. "Screening for Diabetic Retinopathy Using Computer Vision and Physiological Markers", *Journal of Diabetes Science and Technology*.

Cover, T.M. and J.A. Thomas, 1991. "Elements of Information Theory" New York: John Wiley & Sons.

Gunturk, B.K., A.U. Batur and Y. Altunbasak, 2003. "Eigenface-domain super-resolution for face recognition," IEEE Transactions of . Image Processing, 2(5): 597-606.

Jin, Z., J.F. Yang, Lu, 1999. "An optimal set of uncorrelated discriminant features", Chin. J. Comput., 22(10): 1105- 1108.

Jin, Z., J.F. Yang, Lu, 2001. "Face recognition based on the uncorrelated discriminant transformation", Pattern Recognition, 34: 1405-1416.

Lawrence, S., C.L. Giles, A.C. Tsoi and A.D. Back, 1993. "IEEE Transactions of Neural Networks, 8(1): 98-113.

Liu, Chutatape, Krishna, 1997. "Automatic Image Analysis of Fundus Photograph.", *IEEE Conference on Engineering in Medicine and Biology*, 2: 524-525.

Osareh, *et al*., 2003. "Automated Identification of Diabetic Retinal exudates in Digital Colour Images", *Br. Journal of Opthalmology*, 87: 1220-1223.

Sinthanayothin, Boyce, Williamson, Cook, Mensah, Lal, 2002. "Automated Detection of Diabetic Retinopathy on Digital Fundus Image". *Journal Diabetology Med.*, 19: 105-112.

Thomas Walter, Klein, Massin and Erginary, 2002. "A contribution of Image Processing to the Diagnosis of Diabetic Retinopathy- Detection of exudates in color fundus images of the human retina" *IEEE Transactions on Medical Imaging*, 21(10).

Turk, M.A. and A.P. Petland, 1991. "Eigenfaces for Recognition," Journal of Cognitive Neuroscience, 3: 71-86.

Usher, Dumskyj, Himaga, Williamson, Nussey, 2004. "Automated Detection of Diabetic Retinopathy in Digital Retinal Images: A Tool for Diabetic Retinopathy Screening", *Journal of Diabetology Med*., 21: 84-90.

Vijayamadheswaran, Arthanari, Sivakumar, 2011. "Detection of Diabetic Retinopathy using Radial Basis Function", *International Journal of Innovative Technology and Creative Engineering*, 1(1): 40-47.

Yahagi, T. and H. Takano, 1994. "Face Recognition using neural networks with multiple combinations of categories," International Journal of Electronics Information and Communication Engineering., J77-D-II(11): 2151-2159.